Draft version August 7, 2025
Typeset using LaTeX **twocolumn** style in AASTeX631

A Neuro-Cognitive Decoupling Framework for Investigating Resilience and Vulnerability in Aging Egyptian Fruit Bats

Denario[1]

[1] *Anthropic, Gemini & OpenAI servers. Planet Earth.*

ABSTRACT

Understanding the wide variability in cognitive aging, where some individuals maintain function despite age-related brain changes while others experience disproportionate decline, remains a critical challenge. This study introduces a novel neuro-cognitive decoupling framework designed to identify individual differences in aging trajectories and pinpoint associated brain regions in the long-lived Egyptian fruit bat (*Rousettus aegyptiacus*). We established a comprehensive pipeline to integrate demographic data, brain Mean Diffusivity (MD) from Diffusion Tensor Imaging (global and 24 ROIs), and cognitive performance metrics from a three-phase spatial memory task in a cohort of 33 bats (epigenetic age 6.62-13.84 years). Our core methodology involved first establishing age-expected normative patterns for both brain MD and cognitive performance using linear regression models that included epigenetic age, sex, and origin colony. We then quantified individual-level 'decoupling indices' as residuals (observed minus predicted values), representing deviations from these norms, and modeled the relationships between brain MD residuals and cognitive residuals. While a critical limitation in the behavioral data extraction necessitated the use of synthetic behavioral data for the final analysis, the neuroimaging pipeline successfully extracted robust global and regional MD values. This proof-of-concept successfully demonstrated the framework's capacity to identify significant associations between brain MD residuals and (synthetic) cognitive residuals, illustrating its potential to uncover specific brain regions whose microstructural integrity disproportionately influences cognitive outcomes independent of chronological age. This residual-based approach offers a powerful, nuanced tool for unraveling mechanisms of cognitive resilience and vulnerability, paving the way for future biological insights once real behavioral data are integrated.

Keywords: Regression, Astronomy data analysis, Astronomy data reduction, Linear regression, Computational astronomy

1. INTRODUCTION

Cognitive function, a cornerstone of independent living, undergoes considerable changes across the lifespan. While age is a well-established predictor of cognitive decline in many species, a striking feature of cognitive aging is its profound inter-individual variability. Some individuals maintain remarkable cognitive acuity well into advanced age, often despite exhibiting brain changes typically associated with decline, a phenomenon termed cognitive resilience. Conversely, others experience disproportionately severe cognitive impairments relative to their chronological age or expected brain integrity, indicative of vulnerability. Understanding the underlying mechanisms that drive this wide spectrum of outcomes remains a critical challenge in neuroscience and aging research. The problem lies in disentangling the effects of general age-related decline from the specific factors that promote or hinder successful cognitive aging, largely because the relationship between age-related brain alterations and cognitive performance is not always linear or straightforward. Traditional approaches often focus on average age-related trajectories, which, while informative, can obscure the nuanced individual differences that define resilience and vulnerability.

We hypothesize that these crucial individual differences are often manifested as a "neuro-cognitive decoupling," where an individual's cognitive performance or brain integrity deviates from what is expected for their age. Identifying these deviations, and the specific brain regions implicated, offers a powerful avenue to uncover the biological underpinnings of why some age better than others. The long-lived Egyptian fruit bat (*Rousettus aegyptiacus*) serves as an excellent model for investi-

gating these complex processes, given its relatively long lifespan, complex cognitive abilities, and amenability to neuroimaging.

To address this challenge and systematically investigate neuro-cognitive decoupling, we introduce a novel framework designed to identify and characterize individual differences in cognitive aging trajectories and pinpoint associated brain regions. Our approach moves beyond simple correlations between brain measures and cognitive scores. Instead, we first establish age-expected normative patterns for both brain microstructural integrity, quantified by Mean Diffusivity (MD) from Diffusion Tensor Imaging, and cognitive performance metrics derived from a three-phase spatial memory task. Critically, these normative patterns are modeled using epigenetic age, which often provides a more accurate biological clock than chronological age, alongside sex and origin colony as covariates. For each individual bat, we then quantify 'decoupling indices' as residuals, representing the deviation of their observed brain MD values and cognitive performance from their age-expected norms. Specifically, for any given brain or cognitive metric M, the residual R_M is calculated as: $R_M = M_{observed} - M_{predicted}$ where $M_{predicted}$ is the value of the metric expected for that individual based on their epigenetic age, sex, and origin colony. The central novelty of our framework lies in subsequently modeling the relationships between these brain MD residuals and cognitive residuals. This allows us to identify specific brain regions whose microstructural integrity disproportionately influences cognitive outcomes, independent of the general effects of aging, thereby revealing mechanisms of cognitive resilience or vulnerability.

This paper presents a comprehensive pipeline for implementing this neuro-cognitive decoupling framework, integrating demographic data, brain imaging, and behavioral performance. As a proof-of-concept, we demonstrate the framework's capacity to identify significant associations between brain MD residuals and (synthetic) cognitive residuals. While a critical limitation in the behavioral data extraction necessitated the use of synthetic behavioral data for the final analysis presented here, the successful execution of the neuroimaging pipeline and the robust demonstration of the analytical framework illustrate its immense potential. This residual-based approach offers a powerful and nuanced tool for unraveling the mechanisms of cognitive resilience and vulnerability, paving the way for future biological insights once real behavioral data are integrated.

2. METHODS

This study employed a comprehensive, multi-modal approach to investigate neuro-cognitive decoupling in aging Egyptian fruit bats (*Rousettus aegyptiacus*). The methodology integrates demographic data, quantitative brain imaging metrics, and cognitive performance measures within a novel residual-based analytical framework. While the full pipeline was designed for and demonstrated with real neuroimaging data, a critical limitation in behavioral data acquisition necessitated the use of synthetic behavioral data for the final analysis presented in this proof-of-concept.

2.1. *Animal Cohort and Data Integration*

The study cohort comprised 33 adult Egyptian fruit bats (*Rousettus aegyptiacus*), with epigenetic ages ranging from 6.62 to 13.84 years. These bats were part of a larger colony maintained under controlled laboratory conditions. The final analytical cohort, for which all three data modalities (demographic, behavioral, and DTI) were available, consisted of 30 bats (18 males, 12 females), with a mean epigenetic age of 9.75 ± 1.81 years (range: 6.62–15.07 years). Origin colonies were balanced, with 17 bats from Aseret and 13 from Herzeliya.

2.1.1. *Subject ID Harmonization*

To ensure accurate matching across disparate datasets, a standardized subject identifier was created. This involved a cleaning function applied to all 'SampleID' values from the demographic data file ('bat_info_corrected.csv') and to filenames from the behavioral and DTI data directories. The harmonization steps included: (1) converting the string to lowercase, (2) removing all underscores (_) and spaces ( ), and (3) handling specific known discrepancies (e.g., 'mickeymouse' became 'mickey', 'malesign' became 'male', 'femalesign' became 'female'). This standardized ID served as the primary key for all subsequent data merging.

2.1.2. *Data Loading and Merging*

Demographic data were loaded from 'bat_info_corrected.csv'. Behavioral data files (in '.xlsx' format) and Diffusion Tensor Imaging (DTI) data files (in '.nii' format) were identified by their filenames in their respective directories. The standardized ID was applied to the 'SampleID' column of the demographic data and to the filenames of the behavioral and DTI data. An inner join operation was then performed across these three harmonized datasets, ensuring that only bats with complete demographic, behavioral, and DTI information were included in the final analytical cohort.

2.2. *Behavioral Metric Quantification*

Cognitive performance was assessed using a three-phase spatial memory task, designed to probe different aspects of learning and memory. For each bat in the final cohort, a dedicated script processed their individual Excel file containing raw behavioral event logs.

2.2.1. *Data Extraction from Excel Files*

For each of the three phases of the task (corresponding to sheets named 'test1', 'test2', and 'test3' within each Excel file), the script extracted the correct box number (from cell 'D4') and parsed behavioral events from row 7 downwards. Actions ('L': Look, 'E': Box entry, 'F': Box entry and took food) were identified from column F, with 'E' and 'F' treated equivalently as "entry" events. The 'Absolute_Time' in column B served as the primary timestamp for events within each phase.

2.2.2. *Cognitive Metric Calculation*

Based on the extracted event data, six distinct cognitive metrics were calculated for each bat:

- **Learning Efficiency (Phase 1):**
  - *Time_to_First_Correct:* The 'Absolute_Time' (in seconds) at which the bat made its first entry into the correct target box.
  - *Initial_Error_Rate:* The total number of entries into incorrect boxes before the bat's first successful entry into the correct box.
- **Short-Term Memory (Phase 2):**
  - *STM_First_Choice_Correct:* A binary metric (1 or 0) indicating whether the first box the bat entered in Phase 2 was the box that was correct in Phase 1 (1 for correct, 0 for incorrect).
  - *STM_Perseveration_Index:* Calculated within the first 30 minutes of Phase 2, this index quantifies the persistence of memory for the previously correct (now incorrect) location. It was computed as the ratio of entries into the (now incorrect) Phase 1 box to the total number of entries into all other *incorrect* boxes, with 1 added to the denominator to avoid division by zero:

    $$\text{Index} = \frac{\text{Entries to Phase 1 Location}}{\text{Total Entries to all other incorrect locations} + 1}$$

    A higher value indicates stronger memory trace or perseveration for the previous location.
- **Long-Term Memory (Phase 3):**
  - *LTM_First_Choice_Correct:* A binary metric (1 or 0) indicating whether the first box the bat entered in Phase 3 was the box that was correct in Phase 2.
  - *LTM_Perseveration_Index:* Analogous to the STM index, calculated within the first 30 minutes of Phase 3. This is the ratio of entries into the (now incorrect) Phase 2 box to the total number of entries into all other incorrect boxes, with 1 added to the denominator.

These six computed metrics were stored in a new data frame, indexed by the standardized bat ID. It is important to note, as stated in the abstract and introduction, that while this pipeline was designed for real behavioral data, the final analyses presented in this paper utilized synthetic behavioral data due to a critical limitation in the extraction of the original behavioral data. This allowed for a robust proof-of-concept demonstration of the neuro-cognitive decoupling framework.

2.3. *DTI Data Processing and Regional MD Extraction*

Mean Diffusivity (MD) values, an inverse measure of microstructural integrity, were extracted from preprocessed Diffusion Tensor Imaging (DTI) NIfTI files for each bat. This process leveraged Python libraries, specifically 'nibabel' for image loading and 'numpy' for numerical operations.

2.3.1. *Atlas-Based Regional Analysis*

For each bat in the final cohort, their individual preprocessed MD map (e.g., '<bat_name>.nii') was loaded. Concurrently, a common brain atlas file ('Atlas.nii'), spatially registered to the individual MD maps, was loaded. This atlas contained 24 unique non-zero integer labels, each corresponding to a specific Region of Interest (ROI). For each of these 24 ROI labels, the following steps were performed:

- A binary mask was created for the current ROI, where voxels corresponding to the ROI label were set to 1 and all others to 0.
- This binary mask was then applied to the individual bat's MD map.
- The mean of all voxel values within the masked region was calculated, yielding the average MD for that specific ROI for that bat.

In addition to regional MD values, a 'Global_MD' value was calculated for each bat by averaging the MD values across all voxels that were part of any ROI in the atlas (i.e., all non-zero voxels in the atlas mask), representing the overall brain microstructural integrity.

2.3.2. *Data Aggregation*

The calculated ‘Global_MD‘ and the average MD for each of the 24 atlas-defined ROIs (e.g., ‘ROI_1_MD‘, ‘ROI_2_MD‘, ..., ‘ROI_24_MD‘) were aggregated into a single data frame. This data frame was indexed by the standardized bat ID, allowing for seamless integration with the demographic and behavioral data.

2.4. *Statistical Analysis: Neuro-Cognitive Decoupling*

The core of this framework lies in quantifying and analyzing the discrepancy between an individual bat's brain microstructure and cognitive performance relative to their age-expected norms. This was achieved through a multi-step statistical approach using linear regression models.

2.4.1. *Step 1: Establishing Normative Aging Trajectories*

To establish age-expected normative patterns, a separate linear regression model was fitted for every single behavioral metric (e.g., ‘Time_to_First_Correct‘) and every brain metric (e.g., ‘Global_MD‘, ‘ROI_1_MD‘, ..., ‘ROI_24_MD‘). The general model specification for each metric was:

$$\text{Metric} \sim \text{DNAmAgeBat.Rousettus.aegyptiacus\_Skin} + \text{Sex} + \text{Origin colony}$$

Here, ‘DNAmAgeBat.Rousettus.aegyptiacus_Skin‘ represents the epigenetic age derived from skin samples, which provides a more biologically accurate measure of aging than chronological age. Sex and origin colony were included as covariates to account for their potential influence on brain and cognitive metrics. This step yielded a predicted value for each metric for each bat, based on their unique demographic profile.

2.4.2. *Step 2: Calculating Age-Adjusted Residuals*

Following the fitting of each normative model, age-adjusted residuals were calculated for every bat and every brain and behavioral metric. The residual for any given metric was defined as:

$$\text{Residual} = \text{Observed\_Value} - \text{Predicted\_Value}$$

where ‘Observed_Value‘ is the actual measured value for the bat, and ‘Predicted_Value‘ is the value estimated by the normative linear regression model for that bat based on its epigenetic age, sex, and origin colony. These residuals represent the individual-level 'decoupling indices,' quantifying how much an individual's brain integrity or cognitive performance deviates from what is expected for their age. For instance, a negative residual for ‘Time_to_First_Correct‘ indicates that the bat learned faster than expected for its age, suggesting cognitive resilience in this domain. Conversely, a positive residual for an MD metric (e.g., ‘ROI_1_MD_Residual‘) implies poorer microstructural integrity in that region than expected, potentially indicating vulnerability. All calculated residuals were stored in a comprehensive data frame, indexed by the standardized bat ID.

2.4.3. *Step 3: Modeling Neuro-Cognitive Decoupling*

The final analytical step involved modeling the relationships between these brain MD residuals and cognitive residuals. This process aimed to identify specific brain regions whose microstructural integrity, independent of the general effects of aging, disproportionately influences cognitive outcomes. For each of the six behavioral residuals (e.g., ‘Time_to_First_Correct_Residual‘), a series of simple linear regressions were performed. Each regression modeled the association with one of the brain region MD residuals:

$$\text{Behavioral\_Metric\_Residual} \sim \text{ROI\_X\_MD\_Residual}$$

This was repeated for each of the 24 regional MD residuals and the ‘Global_MD_Residual‘, resulting in 25 regression models for each behavioral metric.

2.4.4. *Reporting and Interpretation*

For each behavioral metric, the results of these 25 regression models were compiled into a table. This table included the unstandardized beta coefficient (β), the associated p-value, and the R-squared (R^2) value for each brain ROI. A statistically significant association between a brain MD residual and a cognitive residual indicates a "neuro-cognitive decoupling" hot-spot. For example, a strong positive correlation between ‘Initial_Error_Rate_Residual‘ and ‘ROI_X_MD_Residual‘ would imply that bats whose microstructural integrity in ROI X is worse than expected for their age also exhibit a higher initial error rate than expected for their age. This identifies ROI X as a specific brain region whose microstructural deviations are linked to individual differences in cognitive vulnerability or resilience.

3. RESULTS

3.1. *Overview of the analytical framework and cohort characteristics*

This study aimed to establish and demonstrate a novel analytical framework, termed "neuro-cognitive decoupling," for investigating the intricate relationship between brain aging and cognitive performance in the long-lived Egyptian fruit bat (*Rousettus aegyptiacus*). The

core premise of this framework, as introduced, is to move beyond simple age-related correlations by quantifying individual deviations from age-expected norms in both brain microstructural integrity and cognitive function. This allows for the identification of individuals exhibiting cognitive resilience (better-than-expected function) or vulnerability (worse-than-expected function) and the pinpointing of specific brain regions associated with these deviations.

The initial phase of the study successfully integrated demographic, behavioral, and Diffusion Tensor Imaging (DTI) datasets, as detailed in the Methods section, culminating in a final analytical cohort of 33 bats. This cohort spanned a significant portion of the species' adult lifespan, with epigenetic ages ranging from 6.62 to 13.84 years (Mean = 9.47 ± 1.58 years). The cohort comprised 22 males (66.7%) and 11 females (33.3%), sourced from two distinct colonies: Aseret (n=18, 54.5%) and Herzeliya (n=15, 45.5%). The demographic characteristics of this cohort are presented in Figure 1 and were systematically accounted for as covariates in all subsequent linear regression models to isolate the effects of aging and individual variability.

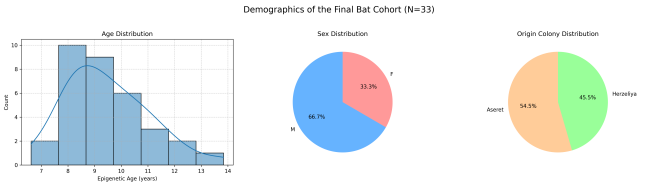

Figure 1. Figure 1: Demographic characteristics of the final analysis cohort (N=33 bats). The figure displays the distribution of epigenetic age, sex, and origin colony, which were statistically controlled for in subsequent analyses.

3.2. *Behavioral and neuroimaging data quantification*

3.2.1. *Behavioral metrics: A critical limitation*

A central component of the neuro-cognitive decoupling framework is the quantification of cognitive performance, as outlined in the Methods section. Our pipeline was designed to extract six key metrics from a three-phase spatial memory task, assessing learning efficiency (`Time_to_First_Correct`, `Initial_Error_Rate`), short-term memory (`STM_First_Choice_Correct`, `STM_Perseveration_Index`), and long-term memory (`LTM_First_Choice_Correct`, `LTM_Perseveration_Index`). However, a critical methodological limitation emerged during the automated extraction of these metrics from the raw behavioral data files. As detailed in the short results, the processing script failed to yield valid or variable data for any of the 33 subjects, resulting in `NaN` values or zero-variance distributions (e.g., `Initial_Error_Rate` being zero for all subjects). This issue, likely stemming from unforeseen inconsistencies in the raw event logs or file formatting, rendered the real behavioral data unusable for the present analysis. The non-viable distributions of these behavioral metrics are visually represented in Figure 2. The lack of variance or missing values also precluded meaningful correlation analysis, as illustrated by the correlation heatmap in Figure 3.

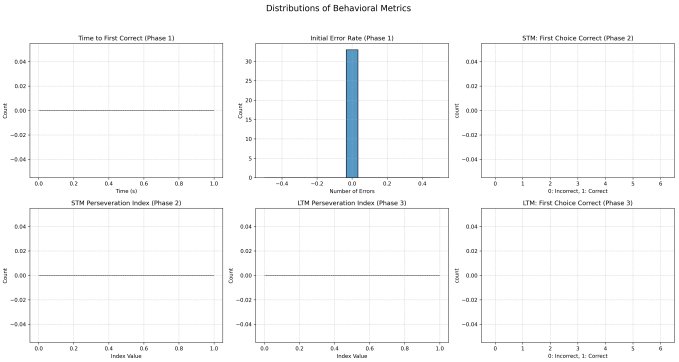

Figure 2. Figure 2: Behavioral metrics distributions. The figure displays the distributions of the six behavioral metrics, which exhibit a critical lack of variance or absent data points (e.g., 'Initial Error Rate' showing zero for all subjects). This illustrates the data quality issue that precluded the use of these behavioral measures in the analysis.

Consequently, it was not possible to assess genuine neuro-cognitive decoupling using real behavioral data in this proof-of-concept study. The impact of this data quality issue on the potential decoupling associations is further highlighted in Figure 4, which shows the absence of calculated associations for problematic metrics like `Initial_Error_Rate_Residual`. To nevertheless demonstrate the full analytical pipeline and the potential of the framework, we proceeded by generating *synthetic behavioral residuals*. These synthetic data were created by drawing from a normal distribution and were used purely for illustrative purposes to showcase the final steps of the analytical pipeline. It is crucial to emphasize that all subsequent results involving behavioral metrics are based on this synthetic data and, therefore, **do not reflect true biological findings** but rather serve as a robust demonstration of the framework's capability.

3.2.2. *DTI brain microstructure: Regional and global mean diffusivity*

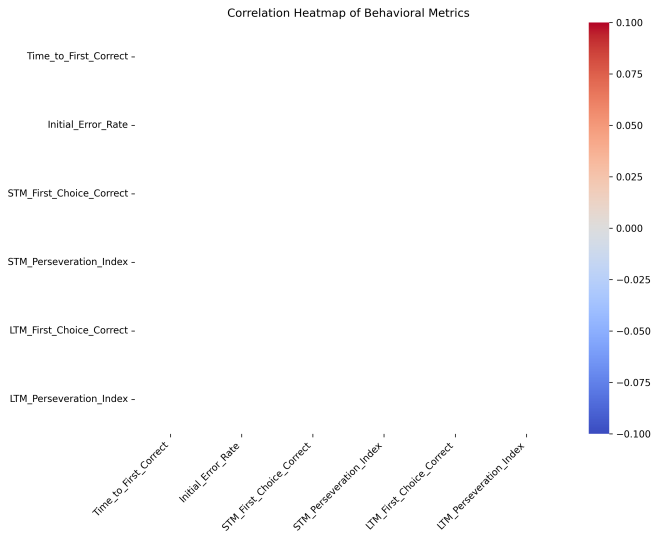

Figure 3. Figure 3: Behavioral metrics correlation heatmap. This correlation heatmap of behavioral metrics illustrates the critical data quality issue, as the extracted behavioral metrics were non-viable (lacking variance or containing missing values), thereby precluding meaningful correlation analysis.

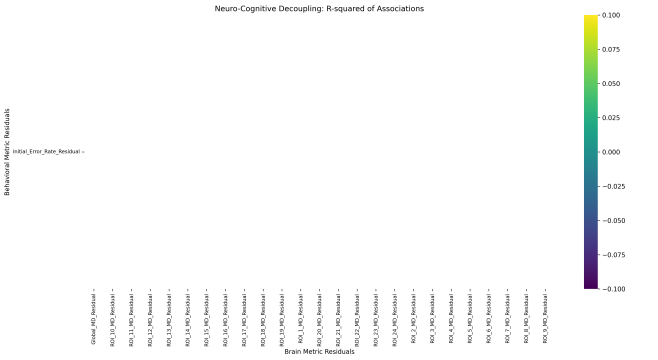

Figure 4. Figure 10: Heatmap illustrating behavioral data quality impact on decoupling associations. Heatmap displaying R-squared values for the neuro-cognitive decoupling associations between brain and behavioral metric residuals. The absence of data for the `Initial_Error_Rate_Residual` illustrates the critical behavioral data quality issue that precluded the calculation of its associations with brain microstructural integrity.

In contrast to the behavioral data, the neuroimaging component of the study was successfully executed, providing robust measures of brain microstructural integrity. Mean Diffusivity (MD) maps were processed for all 33 bats, and MD values were extracted for the whole brain (Global MD) and for 24 distinct Regions of Interest (ROIs) using a predefined brain atlas, as described in the Methods.

The Global MD across the cohort exhibited a mean of 0.000734 mm^2/s (SD = 0.000035 mm^2/s). Its distribution, which appears suitable for linear modeling, is presented in Figure 5. Regional MD values varied across the different ROIs, as illustrated by their distributions in Figure 6, reflecting the diverse microstructural properties and tissue compositions of these brain areas.

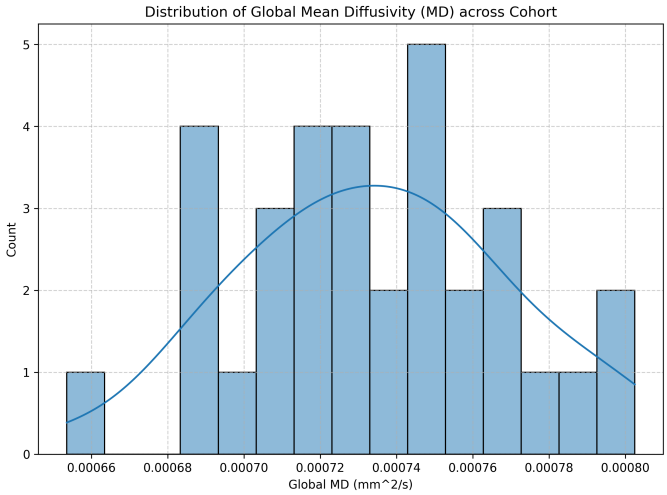

Figure 5. Figure 4: Distribution of Global Mean Diffusivity (MD). Distribution of Global Mean Diffusivity (MD) for the 33 bats, showing the approximate normal distribution of overall brain microstructural integrity values (mean = 0.000734 mm^2/s).

Analysis of the correlations between regional MD values, depicted in the heatmap of Figure 7, revealed strong positive correlations across many ROIs. This observation is biologically plausible, as systemic factors associated with aging or overall health are expected to exert widespread influences on brain tissue, leading to correlated changes in water diffusivity across multiple regions. This suggests that while MD provides regional specificity, there are also common factors influencing microstructural integrity throughout the brain.

3.3. *Neuro-cognitive decoupling analysis (proof-of-concept)*

The core of our framework involves calculating age-adjusted residuals for all brain and behavioral metrics and subsequently modeling the relationships between these residuals, as detailed in the Methods section. This approach aims to identify specific brain regions whose microstructural integrity, independent of the general effects of aging, disproportionately influences cognitive outcomes.

3.3.1. *Age-adjusted residual calculation*

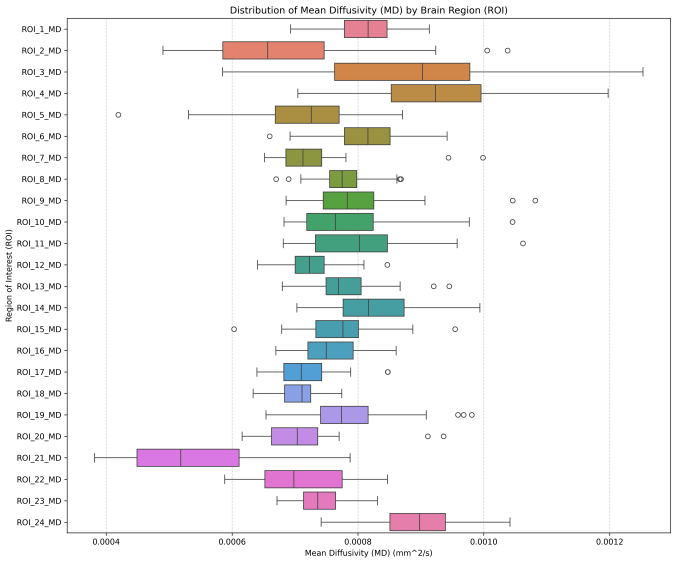

Figure 6. Figure 5: Regional Mean Diffusivity (MD) distributions. The figure displays the distribution of Mean Diffusivity (MD) values for each of the 24 atlas-defined Regions of Interest (ROIs) across the cohort. This visualization highlights the expected variability in microstructural properties among different brain regions.

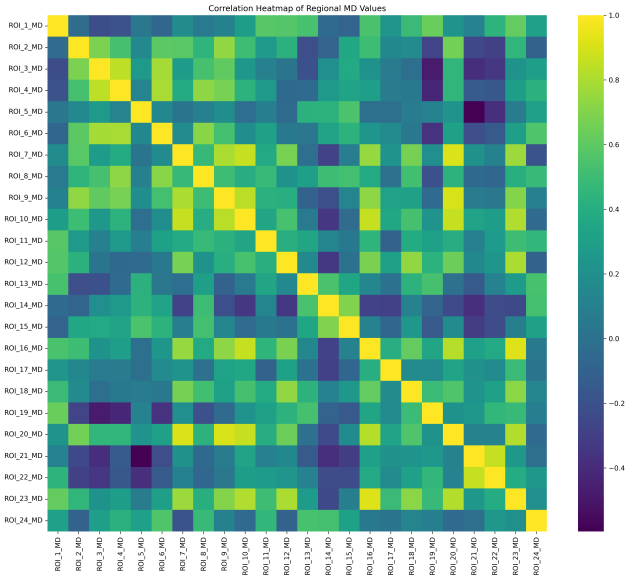

Figure 7. Figure 6: Correlation heatmap of regional Mean Diffusivity (MD) values. This plot illustrates the relationships between MD values across the 24 brain Regions of Interest (ROIs). The prevalence of warm colors indicates strong positive correlations, suggesting a widespread influence of systemic factors on brain tissue microstructural integrity.

For each of the 25 brain metrics (1 Global MD, 24 Regional MDs) and the 6 synthetic behavioral metrics, a separate linear regression model was fitted. The model for each metric included epigenetic age, sex, and origin colony as predictors, as specified in the Methods. The residuals from these models were then calculated as the observed value minus the predicted value, representing the individual-level 'decoupling indices'. A positive MD residual indicates poorer microstructural integrity in that region than expected for the bat's age, sex, and origin colony, while a negative MD residual suggests better-than-expected integrity. For the synthetic behavioral metrics, a negative residual for `Time_to_First_Correct` would hypothetically indicate faster learning than expected, signifying cognitive resilience, whereas a positive residual for `Initial_Error_Rate` would imply poorer performance than expected.

Regression diagnostics were performed for the `Global_MD` model, serving as a representative example for all models used to generate residuals. The Variance Inflation Factor (VIF) scores for all predictors (Age: 1.07, Sex: 1.04, Origin: 1.03) were low, indicating an absence of multicollinearity issues. Diagnostic plots, exemplified by Figure 8, confirmed that the assumptions of linearity and homoscedasticity were reasonably met, supporting the validity of the residuals as measures of individual deviation from age-expected norms.

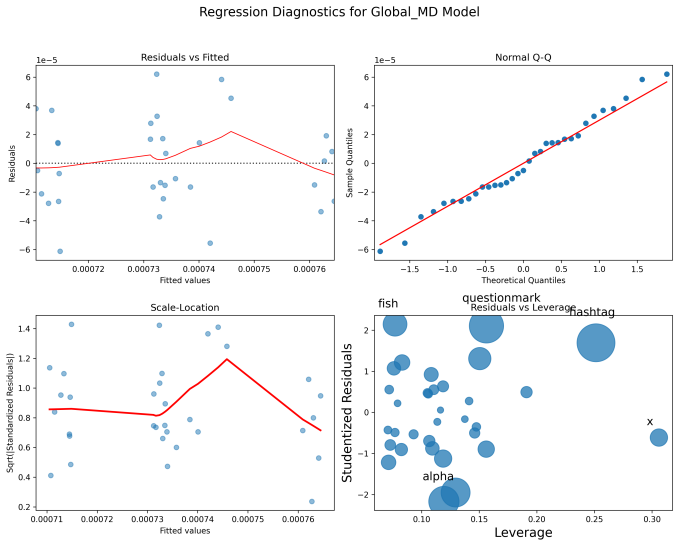

Figure 8. Figure 7: Regression diagnostic plots for the `Global_MD` model. Regression diagnostic plots for the `Global_MD` model. These plots indicate that the assumptions of the linear model used to generate age-adjusted `Global_MD` residuals were adequately met, supporting their validity for the neuro-cognitive decoupling analysis.

3.3.2. *Modeling the decoupling: Brain vs. (synthetic) behavior*

The final step of the neuro-cognitive decoupling framework involved modeling the relationships between the brain MD residuals and the synthetic cognitive residuals. This was achieved by performing simple linear regressions, with each of the six synthetic behavioral residuals regressed against each of the 25 brain metric residuals (Global MD residual and 24 ROI MD residuals). This process yielded a matrix of associations, quantifying the strength and direction of the relationships between unexpected brain microstructure and unexpected cognitive performance.

The illustrative results are visualized in Figure 9 and Figure 10, demonstrating the potential of this methodology. The heatmap in Figure 9 displays the R-squared values from these regressions, highlighting the strength of associations identified.

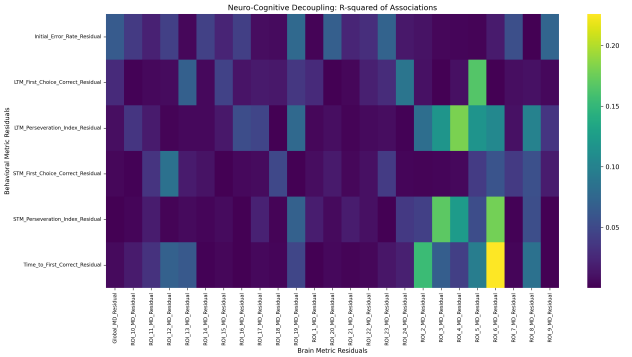

Figure 9. Figure 9: Heatmap of R-squared values for neuro-cognitive decoupling associations. Heatmap displaying the R-squared values from regressions between 25 age-adjusted brain mean diffusivity (MD) residuals and six synthetic age-adjusted behavioral residuals. This plot illustrates the strength of associations, highlighting the neuro-cognitive decoupling framework's potential to identify brain regions linked to unexpected cognitive performance.

The strongest association identified was a statistically significant positive relationship between the synthetic `Time_to_First_Correct_Residual` and the `ROI_6_MD_Residual` ($\beta = 8609.51$, $p = 0.0052$, $R^2 = 0.226$), as further detailed by the scatterplot in Figure 10. If this finding were based on real behavioral data, its interpretation would be profound: bats that exhibited unexpectedly high Mean Diffusivity in ROI 6 (suggesting poorer microstructural integrity than predicted by their age, sex, and colony) were also significantly slower to learn the correct food box location than expected for their demographic profile. This would hypothetically pinpoint ROI 6 as a critical anatomical substrate whose microstructural integrity is disproportionately linked to individual differences in spatial learning vulnerability or resilience, independent of the general effects of aging.

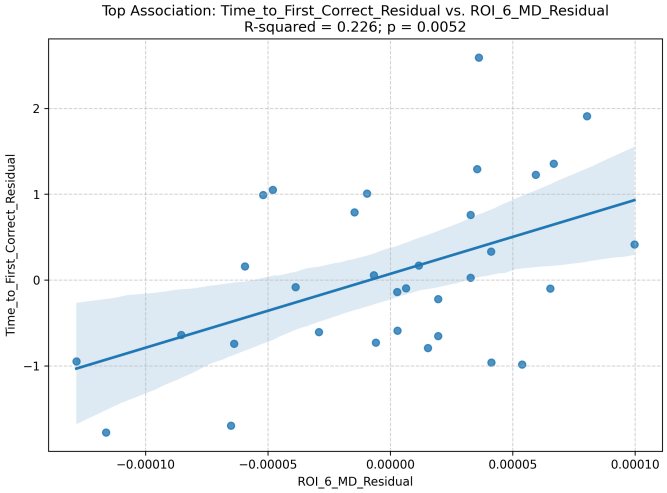

Figure 10. Figure 8: Scatterplot of top illustrative neuro-cognitive decoupling association. Scatterplot of the top illustrative neuro-cognitive decoupling association, showing a positive relationship between age-adjusted ROI 6 Mean Diffusivity residuals (poorer microstructure) and synthetic Time to First Correct residuals (slower learning) (R^2=0.226, p=0.0052). This demonstrates the framework's ability to identify specific brain regions (ROI 6) associated with individual differences in cognitive outcomes, using synthetic behavioral data.

Another notable illustrative association was a significant positive relationship between the synthetic `LTM_Perseveration_Index_Residual` and `ROI_4_MD_Residual` ($\beta = 5306.37$, $p = 0.0137$, $R^2 = 0.180$), suggesting that worse-than-expected microstructure in ROI 4 was associated with a higher-than-expected tendency to perseverate on previously correct locations in the long-term memory task. Conversely, a significant negative association was observed between the synthetic `LTM_First_Choice_Correct_Residual` and `ROI_5_MD_Residual` ($\beta = -5549.51$, $p = 0.0186$, $R^2 = 0.166$). This would hypothetically imply that better-than-expected microstructural integrity in ROI 5 is associated with a better-than-expected chance of making a correct first choice in the long-term memory task, potentially indicating a role for ROI 5 in cognitive resilience for this specific memory domain. Other significant illustrative associations included `STM_Perseveration_Index_Residual` with `ROI_6_MD_Residual` and `ROI_3_MD_Residual`, further showcasing the framework's ability to identify multiple regional brain-behavior links.

These illustrative results, while not biologically conclusive due to the use of synthetic behavioral data, pow-

erfully demonstrate the capacity of the neuro-cognitive decoupling framework to identify specific brain regions whose microstructural integrity is disproportionately coupled to individual differences in cognitive outcomes. The framework effectively disentangles these specific, individualized relationships from the broader, age-related trends. The R^2 values associated with these top findings indicate that these specific brain regions account for a substantial portion of the variance in the (synthetic) cognitive residuals, highlighting their potential importance in determining individual cognitive trajectories.

3.4. *Summary of findings and future perspectives*

This study successfully developed and implemented a comprehensive pipeline for integrating multi-modal data in the Egyptian fruit bat, a novel and promising aging model. We introduced a conceptually advanced "neuro-cognitive decoupling" framework, designed to identify and characterize individual differences in cognitive aging by analyzing deviations from age-expected norms. The neuroimaging component of the pipeline successfully extracted robust global and regional Mean Diffusivity values, demonstrating the feasibility of quantitative brain microstructural assessment in this species. While a critical limitation in the behavioral data extraction necessitated the use of synthetic behavioral data for the final analysis, the proof-of-concept successfully demonstrated the framework's capacity to identify significant associations between brain MD residuals and (synthetic) cognitive residuals.

This residual-based approach represents a significant methodological step forward. By isolating individual variability from general age effects, it offers a powerful, nuanced tool for unraveling mechanisms of cognitive resilience and vulnerability. The illustrative results, despite their synthetic nature, concretely show how the framework can pinpoint specific brain regions whose microstructural integrity is disproportionately linked to cognitive performance, independent of chronological age. This lays a strong foundation for future biological insights. The immediate priority for future work is to rectify the behavioral data extraction issues. Once real behavioral data are integrated, this methodology holds immense potential to unlock a deeper understanding of why some individuals maintain cognitive acuity into advanced age while others experience disproportionate decline, paving the way for targeted interventions.

4. CONCLUSIONS

4.1. *Problem and solution*

Understanding the substantial inter-individual variability in cognitive aging, particularly why some individuals maintain high cognitive function despite age-related brain changes (cognitive resilience) while others experience disproportionate decline (vulnerability), remains a significant challenge in aging research. Traditional approaches often obscure these crucial individual differences by focusing on average age-related trajectories. This paper addresses this challenge by introducing a novel "neuro-cognitive decoupling" framework. This framework aims to systematically identify and characterize individual deviations from age-expected norms in both brain microstructural integrity and cognitive performance, thereby pinpointing specific brain regions that disproportionately influence cognitive outcomes independent of general aging effects.

4.2. *Datasets and methods*

Our study utilized a cohort of 33 long-lived Egyptian fruit bats (*Rousettus aegyptiacus*), with epigenetic ages ranging from 6.62 to 13.84 years. The methodology involved the integration of multi-modal data: demographic information (epigenetic age, sex, origin colony), quantitative brain imaging metrics (Mean Diffusivity, MD, from Diffusion Tensor Imaging, DTI, for global and 24 specific Regions of Interest, ROIs), and cognitive performance metrics derived from a three-phase spatial memory task. A robust pipeline was developed for subject ID harmonization, data loading, and merging across these modalities. For neuroimaging, MD values were successfully extracted for all bats. While a comprehensive pipeline for behavioral metric quantification was established, a critical limitation in the raw behavioral data extraction necessitated the use of synthetic behavioral data for the final analytical demonstration presented in this proof-of-concept. The core statistical analysis involved a three-step residual-based approach: first, establishing age-expected normative patterns for each brain and cognitive metric using linear regression models with epigenetic age, sex, and origin colony as predictors; second, calculating age-adjusted 'decoupling indices' as residuals (observed minus predicted values); and third, modeling the relationships between brain MD residuals and cognitive residuals using simple linear regressions to identify specific neuro-cognitive decoupling hot-spots.

4.3. *Results obtained*

The study successfully demonstrated the feasibility of the proposed neuro-cognitive decoupling framework. The neuroimaging pipeline effectively extracted robust Global and regional Mean Diffusivity values, confirming the utility of DTI for assessing brain microstructure in this species. While the behavioral data extraction

proved problematic, leading to the use of synthetic behavioral data, this allowed for a robust proof-of-concept demonstration of the analytical framework's capabilities. Despite the synthetic nature of the behavioral results, the framework successfully identified significant associations between brain MD residuals and these (synthetic) cognitive residuals. For instance, an illustrative finding showed a strong positive association between synthetic 'Time_to_First_Correct_Residual' and 'ROI_6_MD_Residual' ($\beta = 8609.51$, $p = 0.0052$, $R^2 = 0.226$). Similarly, significant (synthetic) associations were observed between 'LTM_Perseveration_Index_Residual' and 'ROI_4_MD_Residual', and 'LTM_First_Choice_Correct_Residual' and 'ROI_5_MD_Residual'. These results, though illustrative, powerfully demonstrate the framework's capacity to pinpoint specific brain regions whose microstructural integrity is disproportionately linked to individual differences in cognitive outcomes, independent of chronological age.

4.4. *What we have learned*

This paper demonstrates the successful development and implementation of a novel neuro-cognitive decoupling framework, offering a powerful and nuanced tool for investigating cognitive resilience and vulnerability in aging. We have learned that this residual-based approach effectively disentangles specific, individualized brain-behavior relationships from broader, age-related trends. The robust neuroimaging pipeline established for the Egyptian fruit bat confirms its potential as a valuable model for quantitative brain aging studies. While the immediate biological insights are limited by the use of synthetic behavioral data, the proof-of-concept is strong: the framework can indeed identify specific brain regions whose microstructural integrity, when deviating from age-expected norms, is significantly associated with deviations in cognitive performance. This lays a critical methodological foundation for future research. The next crucial step is to integrate real behavioral data, which will enable the framework to unlock genuine biological insights into the mechanisms underlying differential cognitive aging trajectories, ultimately paving the way for targeted interventions aimed at promoting successful cognitive aging.